Electronic Supplementary Material (ESI) for RSC Advances.

Supplementary Information:

Organic-Inorganic Binary Mixture Matrix for Comprehensive Laser-desorption Ionization Mass Spectrometric Analysis and Imaging of Medium-size Molecules including Phospholipids, Glycerolipids, and Oligosaccharides

Adam D. Feenstra[a,b], Kelly C. O'Neill[a], Gargey B. Yagnik[a,b], and Young Jin Lee[a,b]

[a]Department of Chemistry, Iowa State University, Ames, IA 50011, USA

[b]Ames Laboratory-US DOE, Ames, IA 50011, USA

Correspondence to: yjlee@iastate.edu

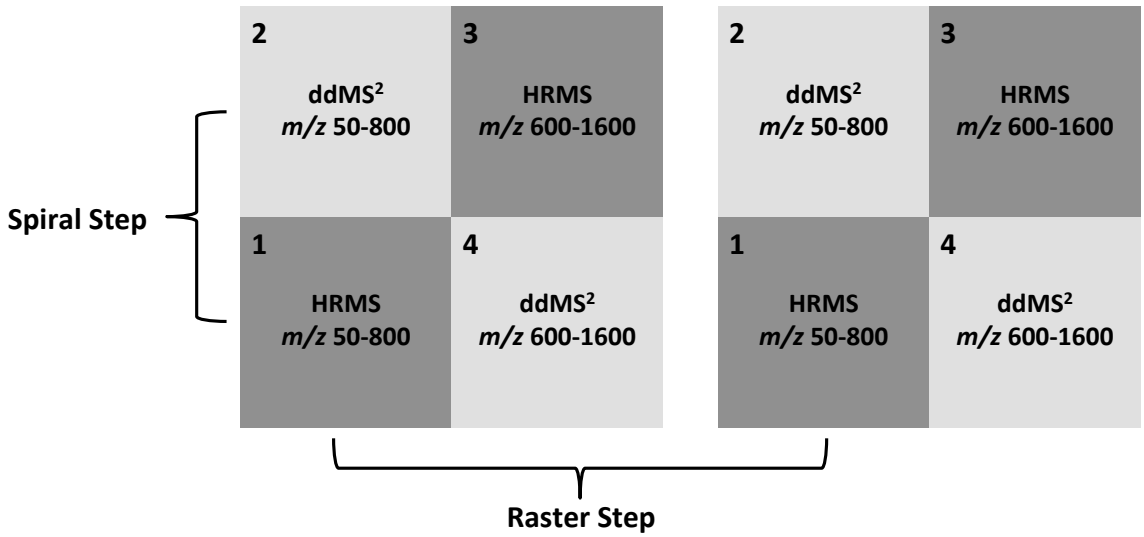

Figure S1. A schematic diagram of the multiplex MS imaging strategy used in this work. In a multiplex data acquisition, each imaging raster step is broken up into multiple spiral steps that can be defined by different MS parameters. In this work, the first and third spiral steps were high resolution Orbitrap scans (HRMS) in the low and high mass range, respectively. The second and fourth steps were data dependent MS/MS scans ($ddMS^2$) from the preceding HRMS scan.

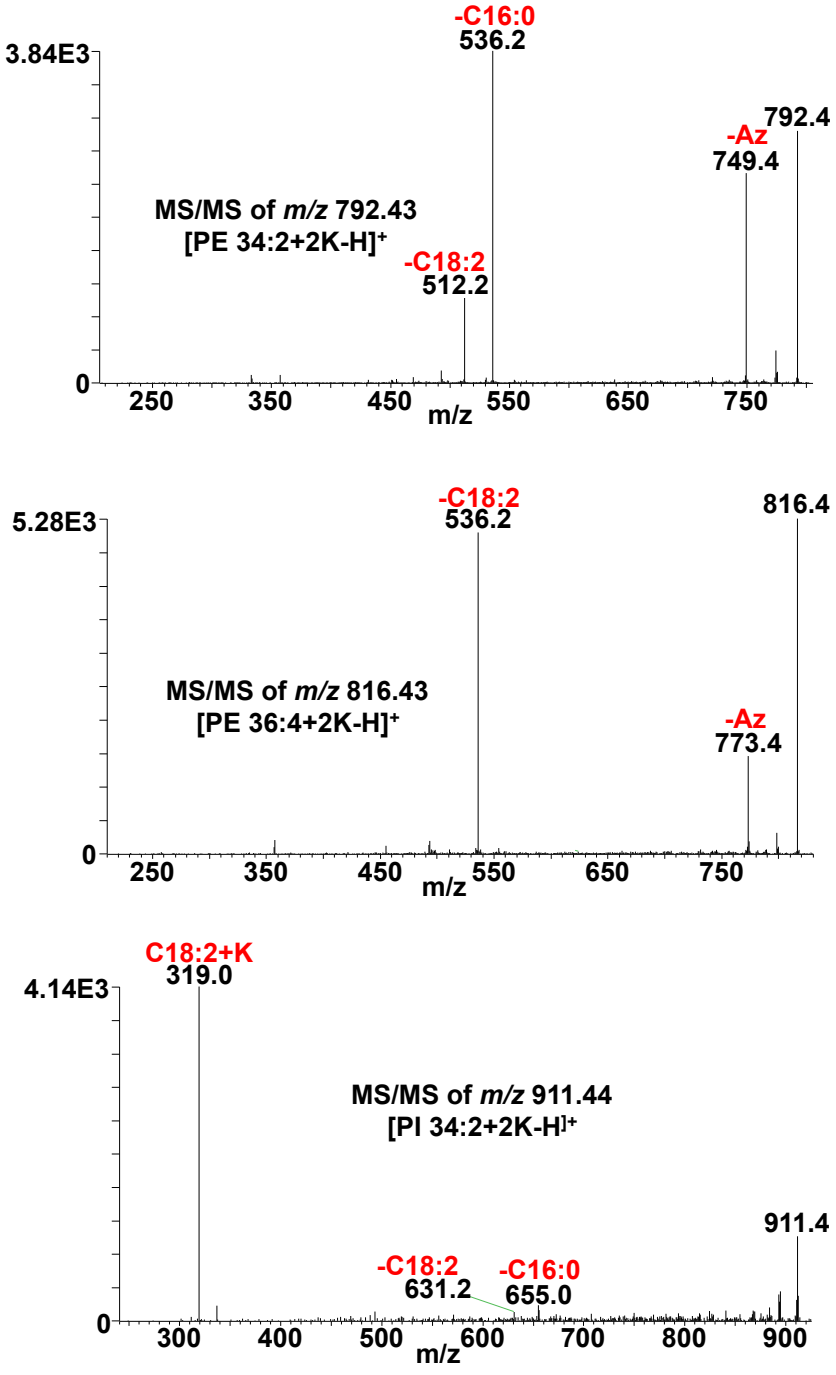

Figure S2. MS/MS spectra for $[PE\ 34:2+2K-H]^+$ (Top), $[PE\ 36:4+2K-H]^+$ (Middle), and $[PI\ 34:2+2K-H]^+$ (Bottom). MS/MS spectra of PEs contain a loss of 43 Da, corresponding to the azidine (Az) fragment previously described by Hsu and Turk (2000, *J Mass Spectrom,* **35**, 596-606). All spectra are from the Fe_3O_4 NP only data set.

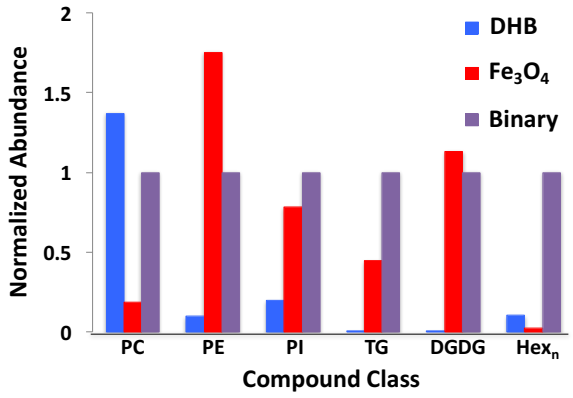

Figure S3. Similar data with Figure 3, but from a separate replicate experiment. Some differences from Figure 3 originate from biological and/or analytical variations.

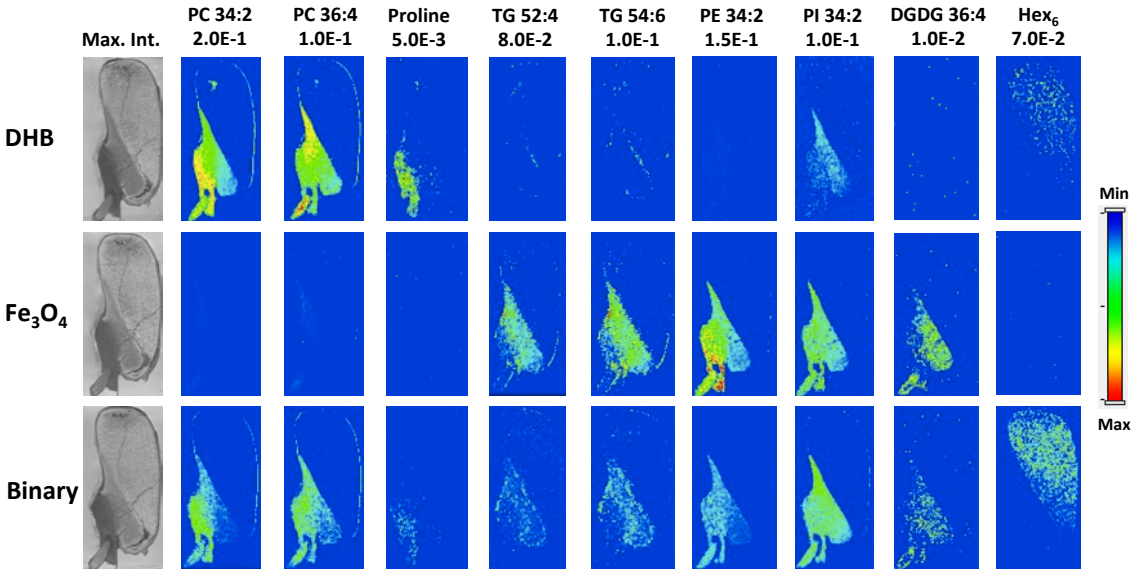

Figure S4. The same MS images as in Figure 4B but generated with normalization to the total ion count. The images demonstrate little to no difference with those generated from absolute ion intensity. Detailed parameters for image generation can be found in Table S2.

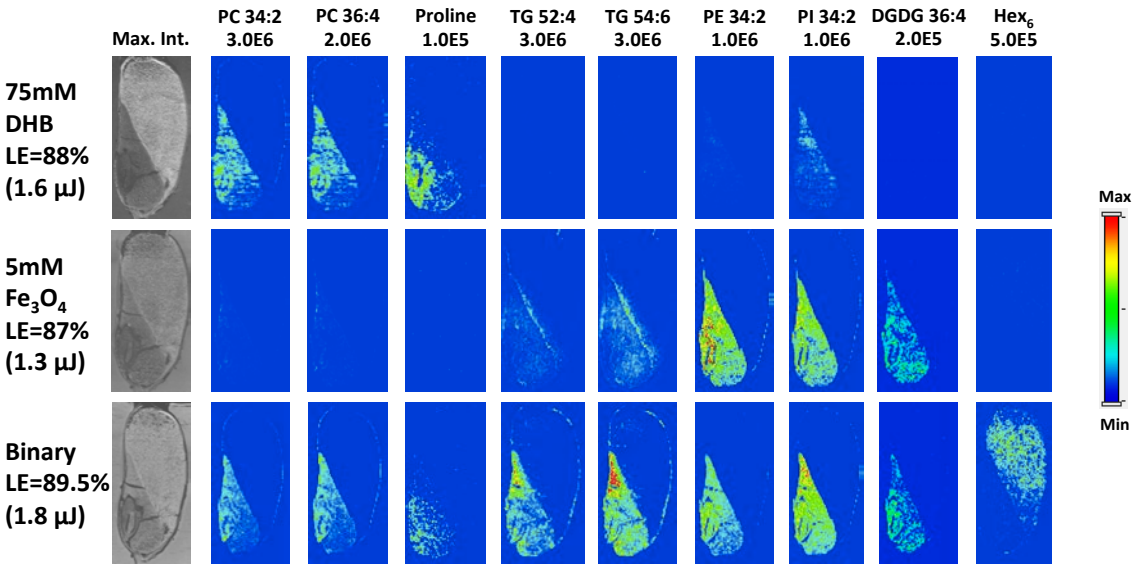

Figure S5. Similar MS images as in Figure 4B but from a separate replicate experiment. Detailed parameters for image generation can be found in Table S2.

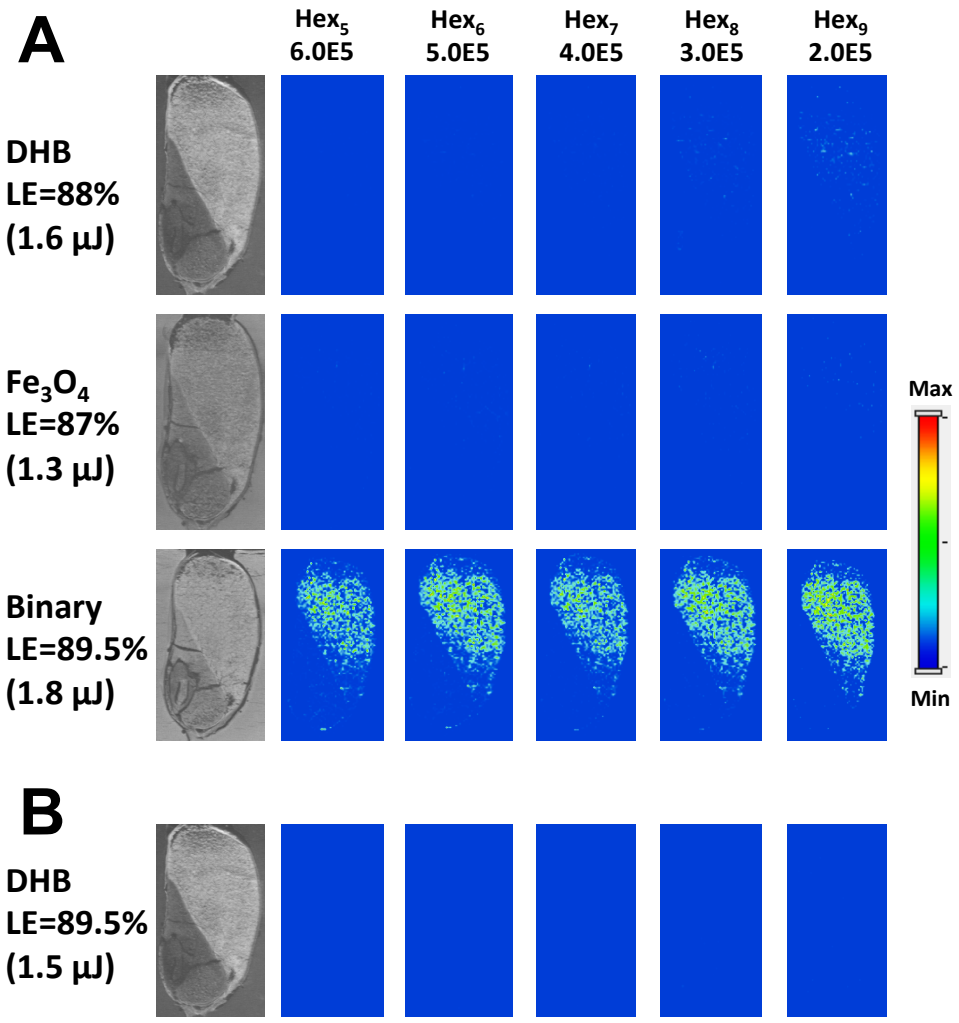

Figure S6. A) Similar MS images as in Figure 5, but from a separate replicate experiment. All species are detected as $[M+K-H_2O]^+$. B) MS images of various polysaccharides with DHB only matrix at the same laser energy as the binary matrix, demonstrating that the high ion signals of large oligosaccharides in the binary matrix is not due to the high laser energy. Detailed parameters for image generation can be found in Table S2.

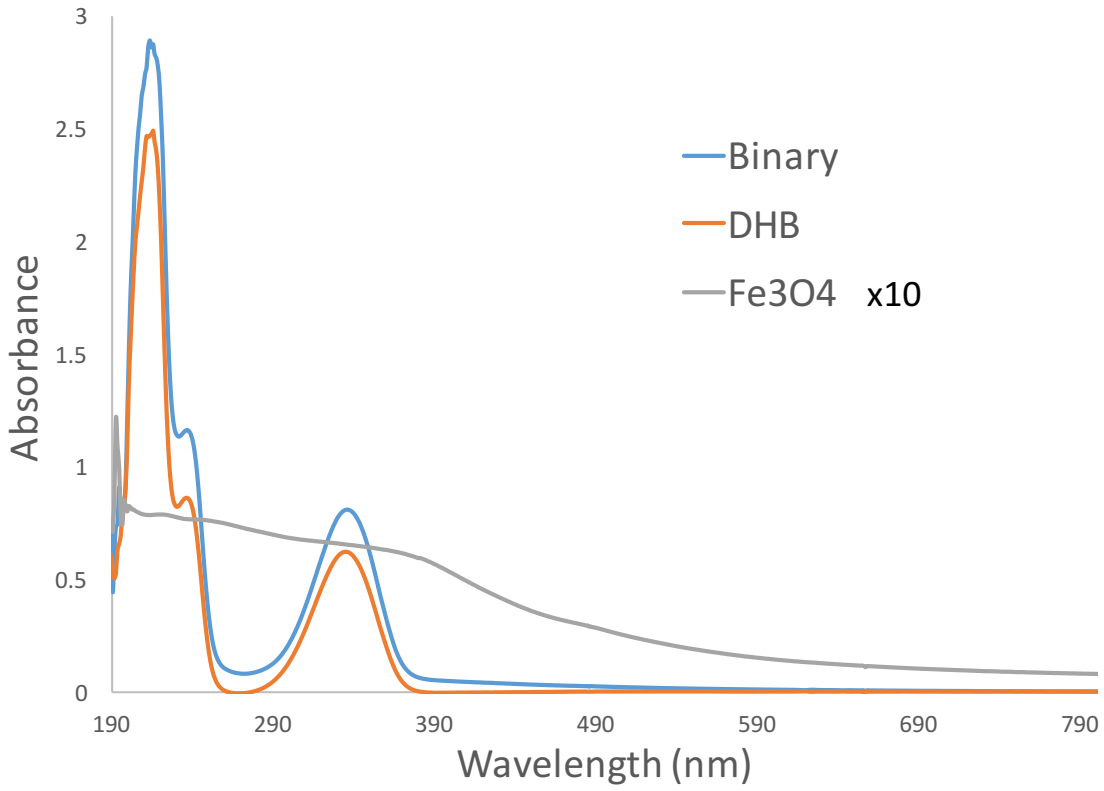

Figure S7. UV-Visible Absorption spectra of DHB, Fe_3O_4 NPs and the binary matrix. DHB and Fe_3O_4 NPs are at the concentration of 0.175 and 0.125 mM, respectively, and the binary matrix contains 0.175 mM DHB and 0.0125 mM Fe_3O_4. This is 400 times dilute concentration than we used in the application to maize seed sections, except the Fe_3O_4 NPs which is 40 times dilute or 10 times more concentrate than used in the UV-Vis of the binary matrix.

Table S1. Assignment of lipid compounds shown in Figure 2.

Accurate mass *m/z*	Identification	Formula	Mass Error (ppm)
737.45024	PC 34:2+K-N$(CH_3)_3$	$C_{39}H_{71}O_8PK$	-2.1
749.39153	PE 34:2+2K-NC_2H_5	$C_{37}H_{68}O_8PK_2$	-0.7
761.45033	PC 36:4+K-N$(CH_3)_3$	$C_{41}H_{71}O_8PK$	-1.9
763.46628	PC 36:3+K-N$(CH_3)_3$	$C_{41}H_{73}O_8PK$	-1.6
775.40824	PC 34:2+2K-N$(CH3)_3$-H	$C_{39}H_{70}O_8PK_2$	0.7
782.56776	PC 36:4+H	$C_{44}H_{81}NO_8P$	-2.1
792.43367	PE 34:2+2K-H	$C_{39}H_{73}O_8NPK_2$	-0.7
796.52383	PC 34:2+K	$C_{42}H_{80}NO_8PK$	-1.9
798.54036	PC 34:1+K	$C_{42}H_{82}NO_8PK$	-0.8
816.43377	PE 36:4+2K-H	$C_{41}H_{73}O_8NPK_2$	-0.6
818.45095	PE 36:3+2K-H	$C_{41}H_{75}O_8NPK_2$	1.3
820.52362	PC 36:4+K	$C_{44}H_{80}NO_8PK$	-2.1
822.54004	PC 36:3+K	$C_{44}H_{82}NO_8PK$	-1.1
824.55610	PC 36:2+K	$C_{44}H_{84}NO_8PK$	-0.6
873.48869	PI 34:2+K	$C_{43}H_{79}O_{13}PK$	-0.3
893.69903	TG 52:4+K	$C_{55}H_{98}O_6K$	-0.5
895.71470	TG 52:3+K	$C_{55}H_{100}O_6K$	-0.5
911.44480	PI 34:2+2K-H	$C_{43}H_{78}O_{13}PK_2$	-0.1
917.69916	TG 54:6+K	$C_{57}H_{98}O_6K$	-0.4
919.71467	TG 54:5+K	$C_{57}H_{100}O_6K$	-0.5
921.72997	TG 54:4+K	$C_{57}H_{102}O_6K$	-0.9
953.55981	DGDG (34:3)+K	$C_{49}H_{86}O_{15}K$	-0.0
955.57515	DGDG (34:2)+K	$C_{49}H_{88}O_{15}K$	-0.3
957.59055	DGDG (34:1)+K	$C_{49}H_{90}O_{15}K$	-0.6
975.54417	DGDG (36:6)+K	$C_{51}H_{84}O_{15}K$	-0.0
977.55957	DGDG (36:5)+K	$C_{51}H_{86}O_{15}K$	-0.3
979.57579	DGDG (36:4)+K	$C_{51}H_{88}O_{15}K$	0.3
981.59073	DGDG (36:3)+K	$C_{51}H_{90}O_{15}K$	-0.4

Table S2. Parameters used in the generation of MS images.

Compound	*m/z*	Tolerance	Min Intensity	Max Intensity
Figure 4B				
PC 34:2+K	796.525	.035	1.00	8.0E5
PC 36:4+K	820.525	.036	1.00	4.0E5
Proline+H	116.071	.002	1.00	8.0E4
TG 52:4+K	893.700	.041	1.00	4.0E5
TG 54:6+K	917.700	.042	1.00	7.5E5
PE 34:2+2K-H	792.435	.034	1.00	8.0E5
PI 34:2+2K-H	911.445	.041	1.00	6.0E5
DGDG 36:4+K	979.576	.046	1.00	2.0E5
Hex_6+K-H_2O	1011.280	.048	1.00	3.0E5
Figure 5				
Hex_5+K-H_2O	849.227	.037	1.00	2.0E5
Hex_6+K-H_2O	1011.280	.048	1.00	2.0E5
Hex_7+K-H_2O	1173.333	.062	1.00	2.0E5
Hex_8+K-H_2O	1335.386	.079	1.00	2.0E5
Hex_9+K-H_2O	1497.439	.088	1.00	2.0E5
Figure S4				
PC 34:2+K	796.525	.035	0.00	2.0E-1
PC 36:4+K	820.525	.036	0.00	1.0E-1
Proline+H	116.071	.002	0.00	5.0E-3
TG 52:4+K	893.700	.041	0.00	8.0E-2
TG 54:6+K	917.700	.042	0.00	1.0E-1
PE 34:2+2K-H	792.435	.034	0.00	1.5E-1
PI 34:2+2K-H	911.445	.041	0.00	1.0E-1
DGDG 36:4+K	979.576	.046	0.00	1.0E-2
Hex_6+K-H_2O	1011.280	.048	0.00	7.0E-2
Figure S5				
PC 34:2+K	796.525	.035	1.00	3.0E6
PC 36:4+K	820.525	.036	1.00	2.0E6
Proline+H	116.071	.002	1.00	1.0E5
TG 52:4+K	893.700	.041	1.00	3.0E6
TG 54:6+K	917.700	.042	1.00	3.0E6
PE 34:2+2K-H	792.435	.034	1.00	1.0E6

PI 34:2+2K-H	911.445	.041	1.00	1.0E6
DGDG 36:4+K	979.576	.046	1.00	2.0E5
Hex_6+K-H_2O	1011.280	.048	1.00	5.0E5
Figure S6				
Hex_5+K-H_2O	849.227	.037	1.00	6.0E5
Hex_6+K-H_2O	1011.280	.048	1.00	5.0E5
Hex_7+K-H_2O	1173.333	.062	1.00	4.0E5
Hex_8+K-H_2O	1335.386	.079	1.00	3.0E5
Hex_9+K-H_2O	1497.439	.010*	1.00	2.0E5

* Tolerance refers to mass windows used in the generation of MS images. Sufficiently large tolerance is used as to be appropriate for corresponding mass resolution at the given mass. In case of $[Hex_9+K-H_2O]^+$, a narrow tolerance is used to avoid the contribution from a near-by contamination peak.